Photosynthesis Research manuscript No.
(will be inserted by the editor)

Supporting Online Information

Maaike T.W. Milder · Ben Brüggemann · Rienk van Grondelle · Jennifer L. Herek

Received: date / Accepted: date

Abstract Insert your abstract here. Include keywords, PACS and mathematical subject classification numbers as needed.

Keywords First keyword · Second keyword · More

1 Linear spectra

1.1 Site Energies

The site energies are, similarly as in *Prosthecochloris aestuarii*, obtained in several ways: firstly as parameters in a fit of the optical spectra (Vulto et al 1998; Renger and May 1998; Adolphs and Renger 2006), a second approach is to calculate the electrochromic shift of the site energies due to charged amino acids (Adolphs and Renger 2006) in table 1 denoted with 'S'.

Maaike T.W. Milder
AMOLF, Sciencepark 113, 1098XG, Amsterdam, The Netherlands
Tel.: +31-20-6081234
Fax: +31-20-6684106
E-mail: milder@amolf.nl

Ben Brüggemann
Institut für Physik, Humboldt-Universität zu Berlin, Newtonstrasse 15, D-12489, Berlin,Germany

Rienk van Grondelle
Department of Physics & Astronomy, Vrije Universiteit Amsterdam, de Boelelaan 1081, 1081 HV, Amsterdam, Netherlands

Jennifer L.Herek
Optical Sciences Group, Department of Science and Technology, MESA+ Institute for Nanotechnology, University of Twente, 7500AE, Enschede, The Netherlands

Table 1 Pigment site energies of *Chlorobium tepidum* expressed in nm. The annotations M and T stand for approaches taking into account only the monomer (M) or the trimer (T).

BChla	1	2	3	4	5	6	7
(Vulto et al 1998)	806.5	793.7	823.7	814.3	800.0	800.0	804.5
(Renger and May 1998)	780.3	806.1	822.2	799.4	800.4	804.6	796.3
(Adolphs and Renger 2006)-M	803.5	798.7	819.3	810.7	800.6	791.1	803.2
(Adolphs and Renger 2006)-T	805.8	798.1	819.0	811.7	801.3	791.8	803.9
(Adolphs and Renger 2006)-S	804.5	815.3	819.3	804.2	816.7	799.4	812.0

Table 2 Lowest site energy of *Chlorobium tepidum*.

Reference	Exciton energy (nm)	Pigment number
(Vulto et al 1998)	823.7	3
(Renger and May 1998)	822.2	3
(Adolphs and Renger 2006)	819.3	3

1.2 Lowest energy pigment

Since the protein structure of the FMO complex of *Prosthecochloris aestuarii* and *Chlorobium tepidum* are relatively similar (homology of 77%), it is expected that the pigment with the lowest site energy is the same in both species. This 'exit' pigment has an important role in guiding the excitation energy from the FMO complex to the reaction center, it is therefore interesting to see that in both species the tendency is towards pigment number 3 (table 2).

1.3 Exciton nature of the FMO complex; delocalization

Similarly as in *Prosthecochloris aestuarii* the contributions of the individual BChla molecules to an excitonic state can be calculated. Results of such calculations, as performed by a variety of research groups, are shown in the tables 3 and 4, where α runs vertically and i horizontally.

Table 3 Contribution of the individual BChla pigments to the monomer exciton transitions in *Chlorobium tepidum*, amplitudes $C_\alpha(j)$ from (Vulto et al 1998).

transition number	1	2	3	4	5	6	7
1	-0.04	-0.07	0.92	0.37	0.06	0.02	0.01
2	-0.06	-0.03	0.35	-0.82	0.28	0.10	-0.34
3	0.91	0.38	0.07	0.00	-0.10	0.09	-0.01
4	0.08	0.09	0.12	-0.33	0.52	-0.73	0.24
5	0.04	0.04	-0.08	0.18	0.39	-0.11	-0.89
6	0.09	-0.19	0.01	-0.22	0.68	0.64	0.17
7	-0.38	0.90	0.05	-0.02	0.11	0.18	0.04

Table 4 Contribution of the individual BChla pigments to the monomer exciton transitions in *Chlorobium tepidum*, amplitudes $C_\alpha(j)$ from (Cho et al 2005).

transition number	1	2	3	4	5	6	7
1	0	0	0.8750	0.1149	0.0050	-0.0002	0.0049
2	0	0	-0.1137	0.5971	0.1096	-0.0145	0.1650
3	0.7755	0.2245	0	0	0	0	0
4	0.2245	0	0.0050	-0.0981	-0.1079	-0.0295	0.7594
5	0	0	0.0048	-0.1262	0.4529	-0.4161	0
6	0	0	0.0015	-0.0637	0.3245	0.5397	0.0706
7	0.2245	0.7755	0	0	0	0	0

Table 5 Exciton energies of *Chlorobium tepidum* in nm.

Exciton transition	A	B	C	D
1	825.6	825.6	825.4	823.7
2	815.5	815.4	814.4	812.0
3	809.4	810.1	808.8	806.5
4	805.4	803.2	805.4	805.2
5	803.3	795.8	803.1	802.6
6	793.0	784.7	796.9	800.0
7	790.6	775.6	792.4	796.2

Where A is from (Vulto et al 1998); B is from (Renger and May 1998); C is from (Abramavicius et al 2008a); and D is from (Abramavicius et al 2008b).

1.4 Coupling strengths, linewidth and exciton energies

Renger and May included dynamic fluctuations of the BChla site energies due to the protein environment, i.e. homogeneous linewidth of the transitions, in their exciton simulations (Renger and May 1998) (see table 5). The authors make use of the point-dipole approximation, taking into account that the smallest interpigment distance is 11 $\AA$. The vibrations in the protein occur on a timescale much slower than the decay of the excitonic system that occur via emission of vibrational quanta. To account for this effect static disorder was introduced in the model. The coupling between the pigments and the bath, consisting of the faster protein and the intramolecular vibrations, is small enough to use a perturbative approach. The linear absorption spectrum was fitted to obtain the necessary input parameters to solve the exciton Hamiltonian. A simplex algorithm was used to find the best fit of the spectra at 5 and 107 K. Plotting the spectral density versus the differential energy clearly shows that the transitions between neighboring exciton states (e.g. 3–4) lie in a spectrally dense area, while transitions across a state (e.g. 3–5) occur in an area with a much lower density. The probability of the latter process is therefore lower and the exciton relaxation is likely to happen step-by-step down the energetic ladder as in *Prosthecochloris aestuarii* (see for examples figure 1). The quality of the fit shows the importance of homogeneous linewidth and the delocalization of the vibrations, that from the fits seems to span the whole trimer. Exciton simulations by Vulto *et al.* were based on the previously successful simulations in *Prosthecochloris aestuarii* by Louwe *et al.* (Louwe et al 1997). These lie also at the basis of simulations of Abramavicius *et al.*. Subsequent simulations from the same authors were based on the refined Hamiltonian by Brixner *et al.* (Abramavicius et al 2008b; Brixner et al 2005).

1.5 Variable fluorescence in the FMO complex-redox effects

Right from the start it was noticeable that there was a difference in optical properties between oxidized and reduced FMO complexes (Miller et al 1994). Reduction can be achieved using a freshly made solution of sodium ascorbate. The oxidized species of the FMO-RC complex (Miller et al 1994) can be obtained chemically by treatment with ferricyanide or by illuminating, an ascorbate reduced complex, with strong white light. At room temperatures the fluorescence increases by a factor of 3-5 upon reduction of the complex (Zhou et al 1994). Because the X-ray structure does not show any redox sensitive groups, oxidized quinones for example are excellent quenchers of excitation energy, the origin of the quenching mechanism remains unknown. The redox effects were visible, both in the steady state spectra and in time-resolved measurements, where the excited state decayed back to the ground state with 60 ps and 2 ns time constants under oxidized or neutral and reduced conditions respectively (Gulbinas et al 1996). The effect of light on three species of green sulfur bacteria was also the topic of a fluorescence study (Hohmann-Marriott and Blankenship 2007). After increasing the amount of illumination, the fluorescence yield shows a rapid increase, after which it slowly decreases on a timescale of minutes. The modulation of the fluorescence is mainly observed in the wavelength regime of the FMO complex, i.e. around 800 nm. However still the exact origin remained unclear. Two proposed mechanisms are direct quenching in the FMO complex, through structural changes, or an indirect mechanism in which the redox state of electron carriers in the RC influence the FMO complex.

However, changes in fluorescence can also have a different origin as was shown in a temperature dependent study of the fluorescence in the FMO complex (Rätsep and Freiberg 2007). The fluorescence intensity starts to decrease from 2 K onwards to room temperature. Addition of glycerol (cryo-solvent) or dithionite to the sample affected the extent of the quenching, but did not stop or alter the nature of the process. A difference fluorescence line narrowing technique was used to determine the origin of the quenching. The authors found that the origin of the quenching must lie in the 825 nm absorption band, because that is where a sharp decrease of the electron-phonon coupling occurs. An exciton explanation for this sharp decrease within the 825 nm band is favored above the explanation of energetically coupled individual BChla molecules.

In short, although several mechanisms are put forward, there still is a lack of an accepted explanation for the quenching of fluorescence within the FMO complex.

2 Nonlinear Spectra and dynamics

2.1 Hole burning

Pressure dependent hole burning experiments showed that the excitonic band at 825 does not change with pressure at 4.2 K. The dephasing time, corresponding to the measured hole widths, is equal to 35 ps in all cases (Reddy et al 1995). Reddy *et al.* give two explanations for the observed decay: electron-phonon coupling destroys the C_3 symmetry and the excitation is trapped on one subunit with a rate of 35 ps, secondly dephasing could occur due to equilibration between split levels in the 827 nm exciton state induced by low-frequency phonons.

2.2 Pump-probe and photon-echo

Room temperature pump-probe experiments with an increased time resolution refined the findings of the earlier experiments on *Prosthecochloris aestuarii* (Savikhin et al 1994). One color experiments showed a 450 fs decay at 796 nm together with a time constant of several tens of ps (table 6), the latter was also observed at 821 nm. The femtosecond component was assigned to downward energy transfer to lower exciton levels. Two color experiments, 800 nm pump and 820 nm probe, showed a rise-time of 350 fs which was taken to be directly related to the decay time at higher energies in the one color experiments. These combined results indeed proved that downward energy transfer from higher excitonic states occurs on a timescale of 100's of fs (Savikhin and Struve 1994) (table 7). Additional experiments by the same authors revealed that the ultrafast components ranged from 100–900 fs depending on pump and probe wavelengths. A comparison between room and low temperature pump-probe experiments showed the slowing down of some of the decay processes from several 100's of femtoseconds at 300 K to 10 ps at 19 K (Savikhin and Struve 1996) (table 8). However, even at these low temperatures some femtosecond processes still occur. Global fitting of pump-probe spectra of *Chlorobium tepidum* at 19 K resulted in several observed time constants; 170 fs, 630 fs, 2.5 ps, 11 ps, 74 ps, and 840 ps (figure 1).

Gulbinas *et al.* did pump-probe measurements on longer timescales in which they found three major time components using global analysis (Gulbinas et al 1996). The two longest time components depended on the addition of a reducing or oxidizing agent during the sample preparation (table 9). At room temperature, the fits resulted in decay times of 7 ps, 60 ps and 2000 ps. At 77 K, similar time constants showed up, 7.4 ps, 104 ps and 1020 ps. When plotting the amplitudes of the different decay components a 26 ps time constant was found and attributed to energy transfer from heated pigments to vibrational modes of the protein. Similar results where obtained by analyzing the pump-probe and fluorescence spectra in a range from 6 to 160 K with a combination of global and single-band analysis (Freiberg et al 1997). Three distinct time constants with wavelength dependent sign of their amplitudes where needed to fit the kinetic pump-probe traces: 0.25 $\pm$ 0.15 ps, 1 $\pm$0.2 ps and a decay constant of 150 ps spreading over the whole spectrum assigned to the excited state lifetime (table 10). Low temperature picosecond fluorescence were discussed in terms of solute-solvent interactions and showed four distinguishable time constants: a rise time of 10-20 ps, a fast decay that varied between 7-60 ps and two slower decay times of 200 ps and 2 ns (Freiberg et al 1997). Their respective amplitudes change depending on the detection wavelength. The interaction between solute and solvent is formally described by the relative response function, that depends on the peak energy at a given time in the time dependent emission spectra. The relative response function for the FMO shows changes from 1 ps up to 10 ns. Fitting the curve resulted in four time constants which were linked tentatively to physical processes in the pigment protein complex. Firstly, the fast time constant of 5.4 $\pm$ 1.3 ps was linked to exciton relaxation within a monomer. Secondly, the time constant of 26.7 $\pm$ 7 ps was linked to energy transfer between the different subunits in the complex, this is in agreement with results from anisotropy measurements (vide infra). The two remaining time constants are attributed to solvation effects; in 163 $\pm$ 58 ps the protein trimer configuration relaxes followed by relaxation in the whole system including the protein and its frozen surrounding in 1930 $\pm$ 590 ps.

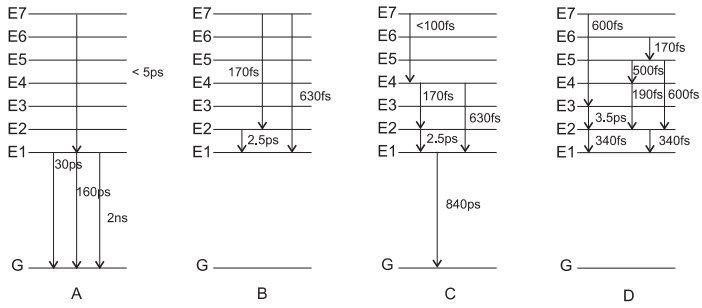

Fig. 1 Proposed relaxation pathways of the exciton energy in the FMO protein. G denotes the ground state and the 7 single exciton levels are represented by E1 through E7. Model A from Freiberg et al (1997), B from Savikhin et al (1997), C from Savikhin et al (1998) and D from Brixner et al (2005).

Savikhin *et al.* were the first to detect oscillations in the anisotropic decay dynamics at 19 K (Savikhin et al 1997, 1998). These oscillations have a period of roughly 300 fs and last up to 1 ps. As the phase of the oscillations is shifted by a factor of π in the parallel and perpendicular polarization traces, they are hardly visible in the isotropic decay dynamics. Refinement of these measurements showed that the period of the oscillations is ∼220 fs which corresponds to 150 cm^{-1}, the energy gap between the 815 and 825 nm band (Savikhin et al 1997, 1998). Due to the fact that the amplitude of the oscillations was dependent on the overlap of the laser with the 815 and 825 nm bands, quantum beating between the two levels was assumed to be the origin of these rapidly dampened (<1ps) oscillations. A mathematical description required the presence of perpendicular transitions within the 815 and 825 nm band, the presence of which were verified by simulations of CD spectra. Simulations by Renger *et al.* confirmed that these oscillations arise from quantum beating between exciton levels are dampened in about 1 ps and have a period of 220 fs (Renger and May 1998).

At higher excitation densities it is possible that exciton energy transfer between single excited monomeric subunits occurs and leads to annihilation of excitations. One way to observe this is in the anisotropy decay of pump-probe experiments. There are only a few reports for singlet annihilation with timescales of 26 ps and 13 ps respectively (Freiberg et al 1997; Savikhin et al 1997) (table 11). Because energy transfer within one monomer occurs as seen above on a much faster timescale (∼ 100 fs) it is likely that the energy transfer between monomers leading to annihilation proceeds mainly between the pigments on which the lowest energy excitons are located. Another way of determining the singlet annihilation time constant is by changing the fluence in transient absorption spectroscopy. Under high excitation conditions, generating more than one exciton per trimer, the kinetics could be fit with multiple exponents (Gulbinas et al 1996). The amplitude of only one of the components, 7 ps, was found to change upon increasing fluence and therefore must correspond to the energy equilibration between the monomers. Temperature dependent pump-probe spectra showed isotropic decay traces depending on the laser fluence (Savikhin and Struve 1996). Decay rates longer than 10 ps were accelerated, mainly coming from the annihilation of excited singlet states with triplet states that were accumulated due to the high repetition rate in this experiment.

Table 6 Frequency dependent decay times of *Chlorobium tepidum*, room T, one-color experiments from (Savikhin and Struve 1994) [a].

Wavelength (nm)	Time constants (ps)
773	0.011, 0.318, 152
790	0.058, 0.417, 21.8
798	0.047, 0.424, 25.3
806	0.018, 0.253, 13.3
815	0.064, 23.8
825	0.108, 27.6
835	0.066, 22.8

[a] In the case of more experiments per wavelength, the first one stated in the original paper is used in the table.

Table 7 Frequency dependent decay times of *Chlorobium tepidum*, room T, two-color experiments from (Savikhin and Struve 1994) [a].

Wavelength (pump-probe) (nm)	Time constants (ps)
800-830	-0.159 [b], -0.412, 52.5
830-800	-0.228, -0.991, 53.5
790-820	-0.067, -0.348, 47.5
780-810	-0.152, -0.838, 43.1
770-800	-0.405, 45.4
810-780	-0.110, -0.941, 27.1

[a] In the case of multiple experiments per wavelength, the first one stated in the original paper is used in the table. [b] The negative signs in front of the decay times correspond to a rise component.

Table 8 Frequency dependent decay times of *Chlorobium tepidum*, room T, two-color experiments in (Savikhin and Struve 1996) [a].

Temperature (K)	Time constants (ps)
19	-0.64 [b], -3.1, -13, 765
52	-0.92, -7.5, 56, 483
130	-0.64, -4.3, 25, 292

[a] Pump 812, probe 829 nm. In the case of multiple experiments per wavelength, the fits from experiments with 70/100 μW pump-probe power are used in the table. [b] The negative signs in front of the decay times correspond to a rise component.

Table 9 Temperature dependent decay times (ps) of *Chlorobium tepidum* at 77 K and room T, from (Gulbinas et al 1996), results are from global analysis of the data.

τ	298 K	77 K
1	7	7.4
2 [a]	60	104
3 [b]	2000	1020

[a] Oxidized and neutral form of the FMO complex. [b] Reduced state of the FMO complex.

Table 10 Decay times of the lowest exciton level of *Chlorobium tepidum* at 77 K.

Reference	τ (ns)
(Freiberg et al 1997)	0.15, 2
(Savikhin et al 1998)	0.84 (300 K)
(Savikhin and Struve 1994)	0.1
(Gulbinas et al 1996)	0.1, 1

Table 11 Anisotropy decay of *Chlorobium tepidum*.

Reference	decay (ps)
(Savikhin and Struve 1994)	75-135, 1.4-2.0 (298K)
(Savikhin and Struve 1996)	8.4 (19K)
(Savikhin and Struve 1996)	4.5 (28K)
(Savikhin and Struve 1996)	1.9 (52K)
(Savikhin and Struve 1996)	0.5, 3.5 (101K)
(Savikhin et al 1997)	0.140-0.180 (between 815–825 at 19K)

2.3 2D-spectroscopy

Brixner *et al.* started with 2D electronic measurements on the FMO protein (Brixner et al 2005). This technique indirectly reveals the energy transfer pathways by means of the off-diagonal cross peaks in a 2D plot where one axis corresponds to the pump pulse, and one axis to the probe pulse. The dynamics is represented by a change of these peaks depending on the delay time between pump and probe. A model of the 2D spectra was obtained by adjusting the site energies from Vulto *et al.* slightly and by reducing the coupling between BChl 5 and BChl 6 as introduced by (Vulto et al 1998). Further simulations of the spectra employed Förster or modified Redfield theory depending on the coupling strengths (cutoff at 30 cm^{-1}). It revealed two energy decay pathways along exciton levels: $7 \rightarrow 3 \rightarrow 2 \rightarrow 1$ and $6 \rightarrow 5 \rightarrow 4/2 \rightarrow 2/1 \rightarrow 1$ (see figure 1 and tables 12 and 13)(Cho et al 2005). Importantly, in the analysis of the 2D spectra rapid energy transfer between exciton levels can occur without the appearance of cross peaks in the spectra if the corresponding combination of transition dipole moments is small.

To simulate 2D electronic spectra of an ensemble of FMO complexes from *Chlorobium tepidum* a non-perturbative approach in the field strength was used (Brüggemann et al 2007). The signal in different, phase-matched, directions was calculated by summing over an ensemble of distributed molecules. As a result this technique is not limited to the 3rd order in the field, but also higher orders are obtained in their respective phase matched directions. Exciton dynamics of the system were calculated using a multi-exciton density matrix approach including up to two excitons. The cross peaks observed in the experiments by Brixner *et al.* relate via the simulations to relaxation between the following exciton levels: $E_3, E_4, E_5 \longrightarrow E_2$; $E_4, E_5 \longrightarrow E_1$; $E_2 \longrightarrow E_1$ and weaker $E_7, E_6 \longrightarrow E_5 .... E_2$ (see table 14). Under high excitation conditions mainly the two exciton states are populated. The spectrum remains its general shape although it is slightly broader and less structured.

By exciting the FMO complex with a laser pulse that spans several exciton levels a coherent superposition of states is created, analogue to a wavepacket in the vibrational regime. Theory predicts that this coherence manifests itself by beating signals with

Table 12 Transfer times between of the exciton levels of *Chlorobium tepidum* at 77 K from (Brixner et al 2005).

Exciton transition	transfer time (ps)
7-3	0.63
3-2	3.6
6-5	0.17
5-4	0.5
5-2	0.63
4-2	0.19
2-1	0.34

Table 13 Lifetime of exciton states of *Chlorobium tepidum* by exciton calculations in reference (Cho et al 2005).

Exciton Number	total decay time (ps)
1	8.3
2	0.28
3	2.2
4	0.15
5	0.21
6	0.12
7	0.41

Table 14 Transfer times between of the exciton levels of *Chlorobium tepidum* at 77 K in reference (Brüggemann et al 2007)[a].

Exciton transition	transfer time (ps)
7-3	0.16
3-2	2.9
6-5	0.32
5-4	1.2
5-2	0.34
4-2	0.34
2-1	0.22

[a] for direct comparison to the 2D data in the table above, only the rates mentioned by Brixner *et al.* are depicted in the table

frequencies that correspond to the energy difference in the excited exciton states. Indeed this beating appeared in 2D electronic spectroscopy, e.g. in the 825 nm crosspeak the oscillations remained up to 660 fs (Engel et al 2007). Not only are the oscillations visible in the amplitude of the cross peak, they also appear in the shape. The oscillations in the peak width, ratio between the diagonal (inhomogeneous broadening) and anti-diagonal width (homogeneous broadening), are anti-correlated with the oscillations in the amplitude. The protein envelope might play an important role in sustaining the coherence during energy transfer and might even be creating new coherences. To model the energy transfer within the FMO accurately long lasting coherence needs to be taken into account, complicating current models.

References

Abramavicius D, Voronine D, Mukamel S (2008a) Double-quantum resonances and exciton-scattering in coherent 2D spectroscopy of photosynthetic complexes. PNAS 105:8525–8530

Abramavicius D, Voronine D, Mukamel S (2008b) Unravelling coherent dynamics and energy dissipation in photosynthetic complexes by 2D spectroscopy. Biophysical Journal 94:3613–3619

Adolphs J, Renger T (2006) How proteins trigger excitation energy transfer in the FMO complex of green sulfur bacteria. Biophysical Journal 91:2778–2897

Brixner T, Stenger J, Vaswani H, Cho M, Blankenship R, Fleming G (2005) Two-dimensional spectroscopy of electronic couplings in photosynthesis. Nature 434:625–628

Brüggemann B, Kjellberg P, Pullerits T (2007) Non-perturbative calculation of 2d spectra in heterogeneous systems: Exciton relaxation in the FMO complex. Chemical Physics Letters 444:192–196

Cho M, Vaswani H, Brixner T, Stenger J, Fleming G (2005) Exciton analysis in 2D electronic spectroscopy. Journal of Physical Chemistry B 109:10,542–10,556

Engel G, Calhoun T, Read E, Ahn TK, Mančal T, Cheng YC, Blankenship R, GR F (2007) Evidence for wavelike energy transfer through quantum coherence in photosynthetic systems. Nature 446:782–786

Freiberg A, Lin S, Timpmann K, Blankenship R (1997) Exciton dynamics in FMO bacteriochloroplhyll protein at low temperatures. Journal of Physical Chemistry B 101:7211–7220

Gulbinas V, Valkunas L, Kuciauskas D, Katilius E, Liuolia V, Zhou W, Blankenship R (1996) Singlet-singlet annihilation and local heating in FMO complexes. Journal of Physical Chemistry 100:17,950–17,956

Hohmann-Marriott M, Blankenship R (2007) Variable fluorescence in green sulfur bacteria. Biochimica et Biophysica Acta 1767:106–113

Louwe R, Vrieze J, Hoff A, Aartsma T (1997) Toward an integral interpretation of the optical steady-state spectra of the FMO-complex of *Prosthecochloris aestuarii*. 2. exciton simulations. Journal of Physical Chemistry B 101:11,280–11,287

Miller M, Cox R, Olson J (1994) Low-temperature spectroscopy of isolated FMO-protein and a membrane free reaction centre complex from the green sulfur bacterium *Chlorobium tepidum*. Photosynthesis Research 41:97–103

Rätsep M, Freiberg A (2007) Unusual temperature quenching of bacteriochlorophyll *a* fluorescence in FMO antenna protein trimers. Chemical Physics Letters 434:306–311

Reddy N, Jankowiak R, Small G (1995) High-pressure hole-burning studies of the bacteriochlorophyll *a* antenna complex from *Chlorobium tepidum*. Journal of Physical Chemistry 99:16,168–16,178

Renger T, May V (1998) Ultrafast exciton motion in photosynthetic antenna systems: The FMO complex. Journal of Physical Chemistry A 102:4381–4391

Savikhin S, Struve W (1994) Ultrafast energy transfer in FMO trimers from the green bacterium *Chlorobium tepidum*. Biochemistry 33:11,200–11,208

Savikhin S, Struve W (1996) Low-temperature energy transfer in FMO trimers from the green photosynthetic bacterium *Chlorobium tepidum*. Photosynthesis Research 48:271–276

Savikhin S, Zhou W, Blankenship R, Struve W (1994) Femtosecond energy transfer and spectral equilibration in bacteriochlorophyll a-protein trimers from the green bacterium *Chlorobium tepidum*. Biophysical Journal 66:110–114

Savikhin S, Buck D, Struve W (1997) Oscillating anisotropies in a bacteriochlorophyll protein: Evidence for quantum beating between exciton levels. Chemical Physics 223:303–312

Savikhin S, Buck D, Struve W (1998) Towards level-to-level energy transfer in photosynthesis: The Fenna-Matthews-Olson protein. Journal of Physical Chemistry B 102:5556–5565

Vulto S, De Baat M, Louwe R, Permentier H, Neef T, Miller M, Van Amerongen H, Aartsma T (1998) Exciton simulations of optical spectra of the FMO complex from the green sulfer bacterium *Chlorobium tepidum* at 6k. Journal of Physical Chemistry B 102:9577–9582

Zhou W, Lobrutto R, Lin S, Blankenship R (1994) Redox effects on the bacteriochlorophyll-a containing Fenna-Matthews-Olson protein from *chlorobium tepidum*. Photosynthesis Research 41:89–96